Modeling Density Changes Inside a Cryogenic Target using a Fabry-Perot Interferometer: A Feasibility Study

Evan Lustick

Canandaigua Academy

Canandaigua, New York

Advisors: Dr. R. S. Craxton, Mark Wittman

Laboratory for Laser Energetics

University of Rochester

Rochester, New York

October 2012

1. Abstract

The use of a Fabry-Perot interferometer has been proposed as a method of measuring changes in deuterium gas density inside a cryogenic target. It is important to determine whether rapidly decreasing the temperature of the helium gas surrounding the target results in the required change in deuterium gas density for use on the National Ignition Facility. A program, *SAKURA*, has been written to investigate the feasibility of this proposal. *SAKURA* calculates the intensity of the interference fringes based on the distance between the two mirrors that make up the interferometer, the temperature of the target, and other parameters. Multiple bounces between the mirrors and refraction through the target layers are taken into account and interference fringes inside the target as well as background fringes are modeled. *SAKURA* has shown that the interference fringes are experimentally detectable and that a high mirror reflectivity is required. Experiments using the interferometer, along with *SAKURA*, will be used to study the thermal lag of heat out of the target following a sudden drop in ambient temperature.

2. Introduction

Nuclear fusion is a potential source of plentiful clean energy. One method used to achieve fusion is to irradiate a plastic spherical target filled with deuterium and tritium, two isotopes of hydrogen, with high-energy laser beams. This method is referred to as inertial confinement fusion (ICF). The plastic shell ablates, and the inner layers are compressed, resulting in very high pressure and

temperature in the deuterium and tritium. These conditions allow the positively charged nuclei of the inner layers to overcome the repulsive electrostatic forces between them, and fuse. Two nuclei fuse to create a helium nucleus, as well as an energetic neutron. If the mass of fuel inside the target is high enough, the helium nuclei can deposit their energy in the remaining fuel, resulting in more fusion reactions. This is referred to as ignition. If ignition occurs, the energy output of the fusion reactions can exceed the energy input of the laser beams. ICF will be a feasible energy source when the energy produced by the reaction is roughly two orders of magnitude greater than the energy output of the laser. Ignition is only currently possible on the National Ignition Facility (NIF) laser. The NIF is the most powerful laser in the world, delivering 1.8 megajoules on a timescale of a few nanoseconds.

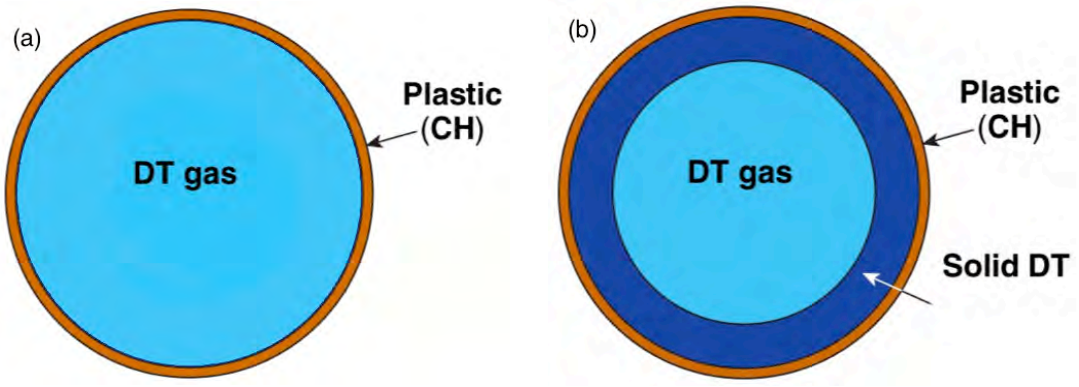

Figure 1: Two main target types used for inertial confinement fusion. (a) A plastic shell encases DT gas. (b) A cryogenic target has a solid DT mantle between its shell and the DT gas core.

There are two main types of targets used for inertial confinement fusion. The first type of target consists of only two layers: a thin plastic shell filled with

deuterium-tritium (DT) [Figure 1(a)]. Cryogenic targets, the second type, consist of a plastic shell with a low density gaseous DT center, but with a relatively thick layer of DT ice between them [Figure 1(b)]. The DT gas density depends on the vapor pressure of the DT ice, which depends strongly on the temperature of the DT ice. A cryogenic target contains a much larger mass of DT, and allows for higher energy output from the same laser energy input. The cryogenic DT ice layer is formed at 19.79 K.[1]

In order to achieve fusion on the NIF, the DT gas in the cryogenic target must have a specific density. To achieve the desired density, the temperature of the helium gas is lowered from 19.79 K to 18.0 K. This leads to a rapid deposition of the gas onto the ice layer, lowering the gas density to the required value. If the target has too large of a thermal lag, and does not cool quickly enough, then the DT ice layer can begin to peel away from the plastic, resulting in an unusable target. The use of a Fabry-Perot interferometer was proposed to confirm that the drop in ambient temperature results in the expected change in gas density. The goal of this work was to produce a computer model of this experiment to test its feasibility. The resulting model, *SAKURA*, has shown that it is feasible to use the proposed method to measure gas-density changes in a cryogenic target for use on the NIF.

3. Experimental Setup

A Fabry-Perot interferometer [2] is a relatively simple device. It consists of two parallel, separated, highly reflective mirrors. The Fabry-Perot device has several applications in interferometry, spectroscopy, and other areas of physics.[3]

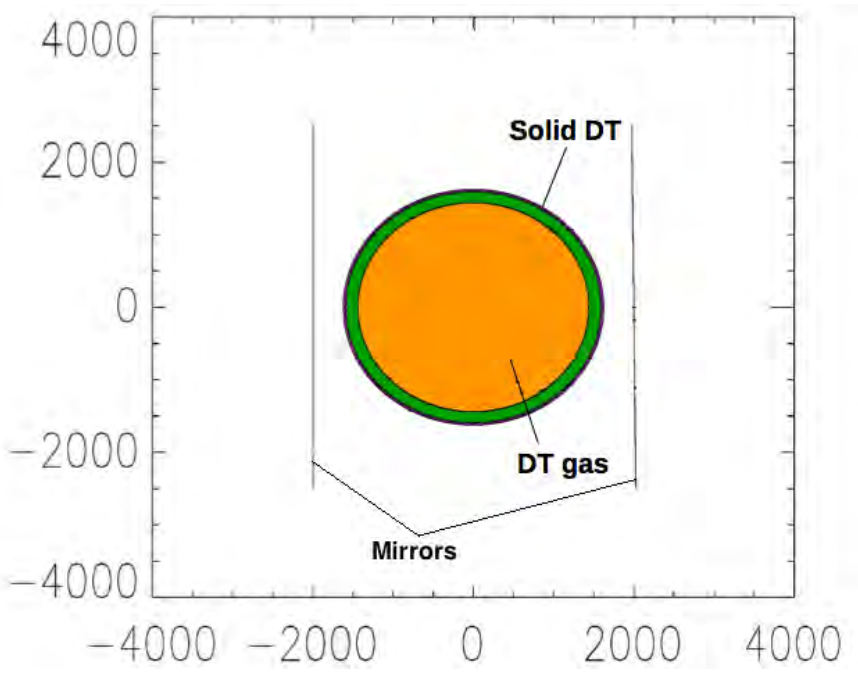

Figure 2: The experimental setup. A cryogenic target is placed in the center of a Fabry-Perot interferometer formed by the two mirrors. Distance in μm is shown on the x and y axes.

In the proposed experiment, which will use D_2 as a surrogate for DT, a cryogenic target is placed between the mirrors of the interferometer, as shown in Figure 2. The interferometer is filled with helium gas. Plane parallel wavefronts from a laser illuminate the interferometer, creating an interference pattern. This pattern is imaged onto a camera by a collection lens, which is oriented opposite the laser. By analyzing the changes in this pattern as the ambient temperature is decreased, one can discern if the desired change in gas density has occurred.

4. Interference Model *SAKURA*

This project entailed writing a program, *SAKURA*, to model the experimental system. *SAKURA* traces a ray of light as it passes through the first mirror, the target, and the second mirror, and records its intensity as it is collected by the lens. It also traces the ray through a given number of bounces between the mirrors, with a new intensity value calculated for every pair of bounces. It traces a few hundred in-phase rays that are just a few microns apart in the vertical direction of Figure 2. This models the behavior of a laser beam with a diameter slightly less than that of the target, which is 3300 μm for a typical NIF target. *SAKURA* collects information that the collection lens would receive to generate an interference pattern. Adjustable parameters in *SAKURA* include the spacing between the two mirrors, the temperature of the target, the wavelength of the laser light, the reflectivity of the mirrors, the tilts of the mirrors, the F-number of the collection lens, and the refractive indices of the plastic, D_2 ice, and D_2 gas. Some adapted segments of previously written code [4] were used. All code was written in the programming language PV-Wave.[5]

4.1 Refraction and Reflection in the Model

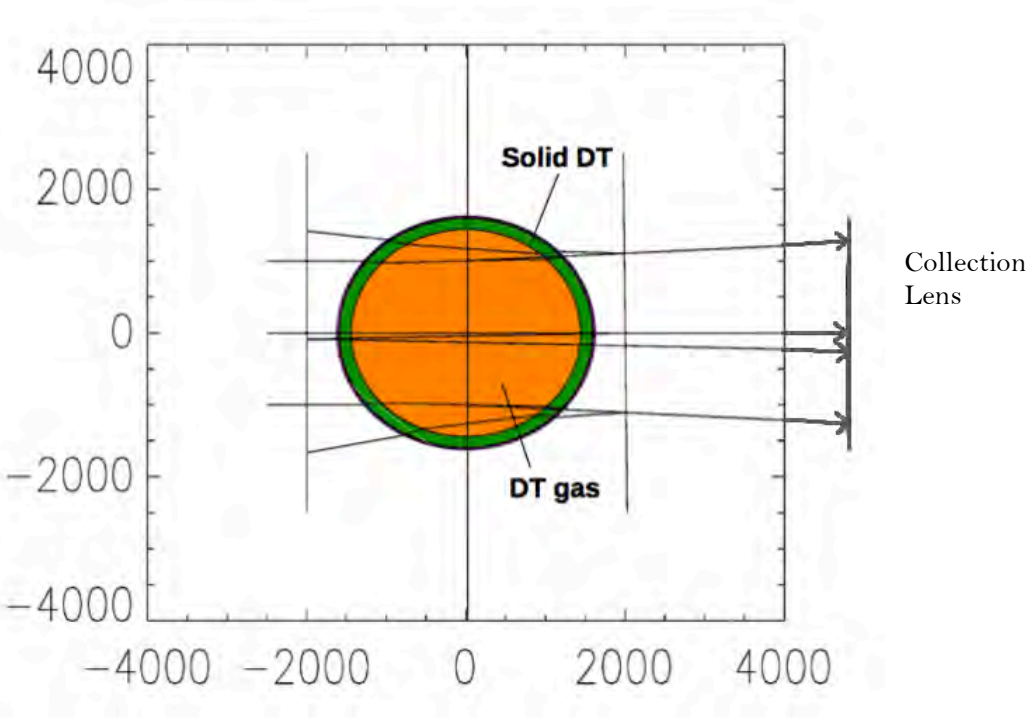

Figure 3: An exemplary run of the code. Three different rays are plotted to show how rays are refracted and reflected within the interferometer. Only one bounce between the mirrors is shown and the rays' paths are extended to the collection lens for ease of viewing. Distance in μm is again shown on the x and y axes.

SAKURA traces rays through the interferometer one at a time. Three rays, shown in figure 3, show how the edges and center of the beam behave within the apparatus. The refraction of the top and bottom rays is clearly visible as they pass through the target, while the center ray hits perpendicular to the surface of the target and does not refract. The reflection of all three rays off the rightward mirror can also be seen, as the right mirror is slightly tilted. The bottom and top rays, however, do not reflect off the leftward mirror in the model, as *SAKURA* recognizes that the reflected ray will not intersect with the target.

SAKURA also recognizes when a ray refracts through the target such that it will miss the lens. Each time a ray reaches the rightward mirror, it is partially reflected, but a beam containing most of its energy continues to the collection lens, where the ray's energy is recorded.

4.2 Primary Intensity Plots

After a ray reaches the collection lens, *SAKURA* traces the ray back to the object plane along the angle at which the ray hits the lens. The object plane is used as a reference plane from which all rays appear to originate and is shown as the central vertical line in figure 3. *SAKURA* calculates the intensity of each ray at its back-traced location on the object plane, then interpolates those intensity values to find several hundred intensity values at regular intervals from the bottom of the image to the top.

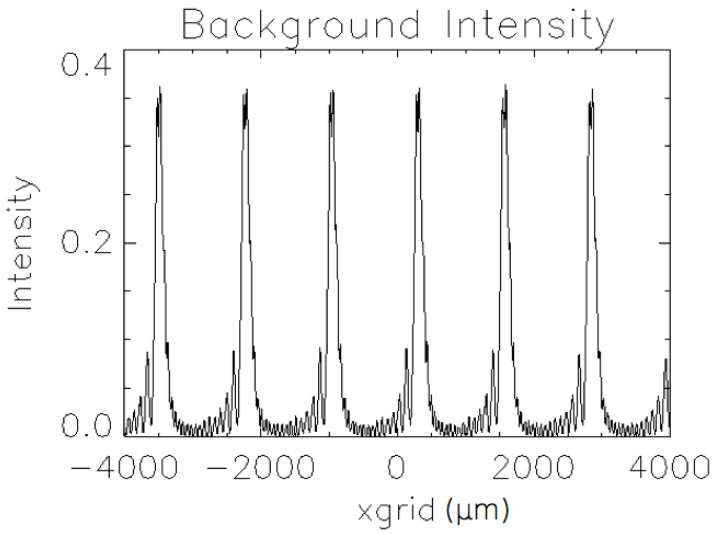

Figure 4: An intensity plot showing background interference fringes, generated with no target present in the Fabry-Perot interferometer. The x-axis shows the interpolated intensity value's location along the vertical direction of figure 3. The y-axis shows intensity as a fraction of the intensity of a beam before it enters the interferometer.

SAKURA plots these intensity values against their calculated position on the object plane. Figure 4 shows the intensity plot generated when the interferometer does not contain a target. The mirrors are 90% reflective, the right mirror is tilted at an angle of 0.57°, and the wavelength of the laser beams is 633 nm. The peaks represent maximum constructive interference between the rays, and the troughs represent maximum destructive interference. The roughness in the pattern between peaks is a result of the slight tilt of the mirrors, which creates areas of relative constructive and destructive interference between the absolute peaks. The plot shown agrees very well with a literature plot of a Fabry-Perot interferometer with slightly skew mirrors.[6]

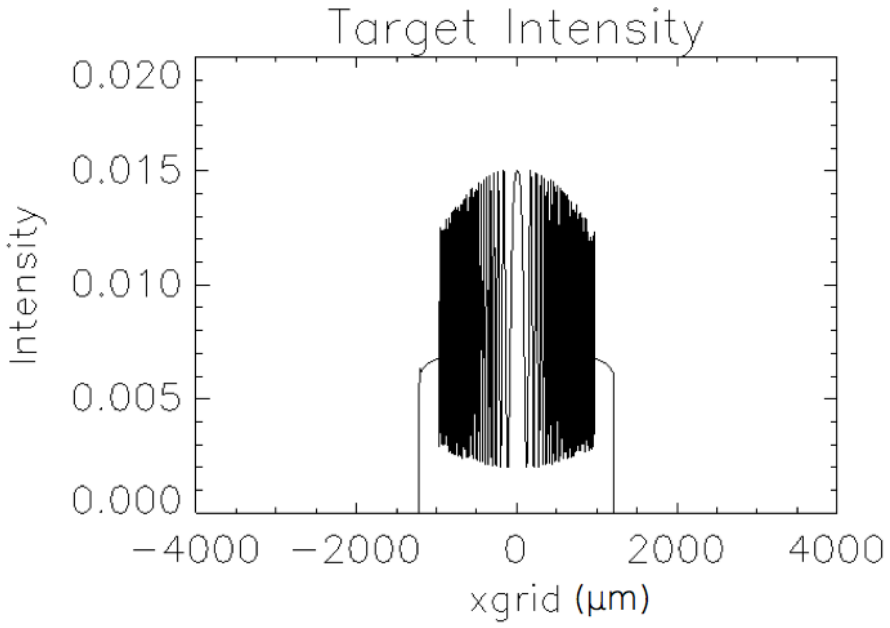

Figure 5: An intensity plot generated only by rays passing through the target. The background intensity plotted in figure 4 is not shown.

A plot showing only the intensity of the back-traced rays that have passed through the target is shown in figure 5. The thickness of the CH shell is 33 μm. The thickness of the D_2 ice is 155 μm. The D_2 gas layer has a radius of 1440 μm. The refractive indices of CH, D_2 ice, and D_2 gas are 1.59, 1.13, and $1 + 3.565 * 10^{-4}$ (at 18.73 K), respectively.[1] The center region of this plot, where relatively little refraction occurs, is the easiest region to interpret for the purposes of the simulation. This is because of the ease of tracking phase changes within the region. For this plot, the distance between the mirrors has been adjusted so that a ray traveling through the center of the target will have an optical path length equal to a whole number of wavelengths, which will result in maximum constructive interference, and thus a peak at the location to which that ray is back-traced. This location is slightly off-center due to the tilt of the second mirror.

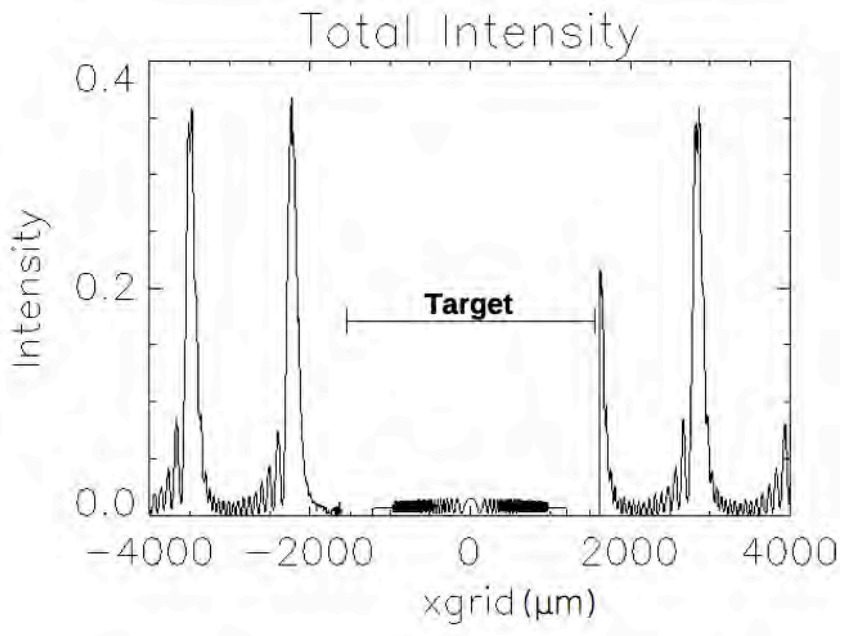

Figure 6: An intensity plot showing the interference pattern generated in the experimental setup, including background fringes and fringes through the target.

An intensity plot for the full experimental setup is shown in figure 6. The background intensity can be seen to smooth out as it approaches the target from the left. This occurs because the target blocks some rays that would normally contribute to the interference pattern in the smoothed area. The areas with zero intensity are where incoming rays never hit the collection lens, as they are refracted at too high an angle. Otherwise, this plot is merely the previous two combined. This plot serves as a base to compare to other plots as the target is cooled.

4.3 Density Change Intensity Plots

As the target is cooled from 18.73 K (the triple point of D_2) to 17.23 K, D_2 gas will deposit on the D_2 ice layer of the target. This will slightly thicken the ice layer, while reducing the density, and thus the refractive index, of the gas in the interior. The gas density drops rapidly as the target is cooled below the triple point. Based on formulae given in Souers,[1] the density drops from $4.529 * 10^{-4}$ g/cm^3 at 18.73 K to $2.115 * 10^{-4}$ g/cm^3 at 17.23 K, and $n - 1$ (where n is the refractive index) drops from $3.565 * 10^{-4}$ to $1.665 * 10^{-4}$. These changes combine to slightly lengthen the optical path taken by a ray traveling through the center of the target. This results in the optical path length being equal to a non-whole number of wavelengths. As a result, the interference in the center of the target intensity plot is no longer totally constructive. Figure 7 shows the changes in the interference plot as the target is cooled.

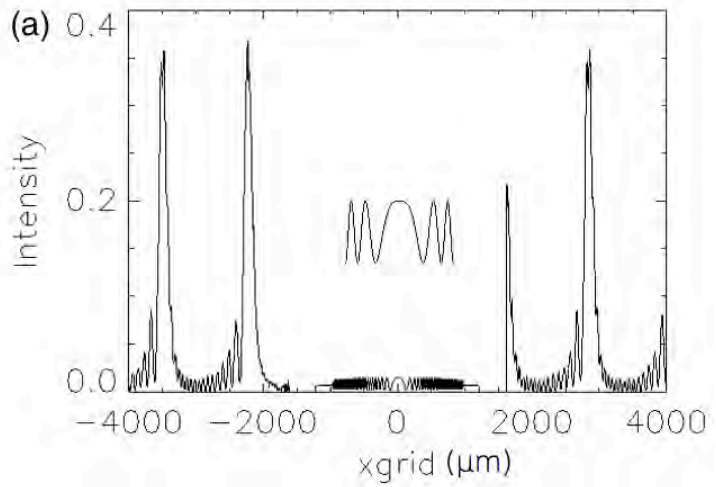
(a)
0.4
0.2
0.0
Intensity
−4000
−2000
0
2000
4000
xgrid (μm)

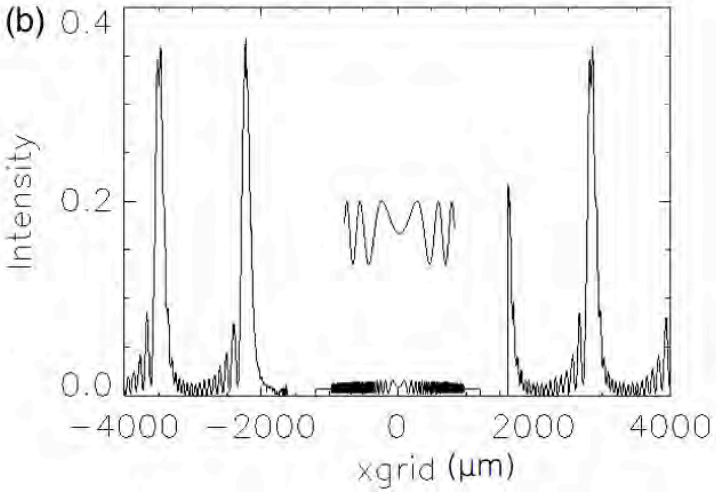
(b)
0.4
0.2
0.0
Intensity
−4000
−2000
0
2000
4000
xgrid (μm)

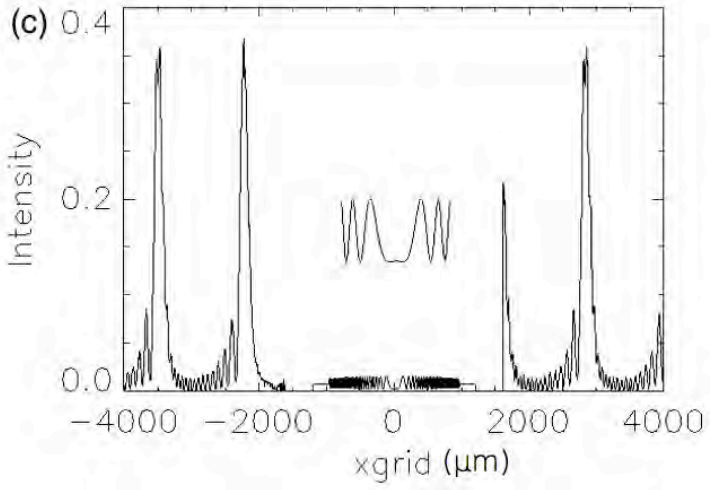
(c)
0.4
0.2
0.0
Intensity
−4000
−2000
0
2000
4000
xgrid (μm)

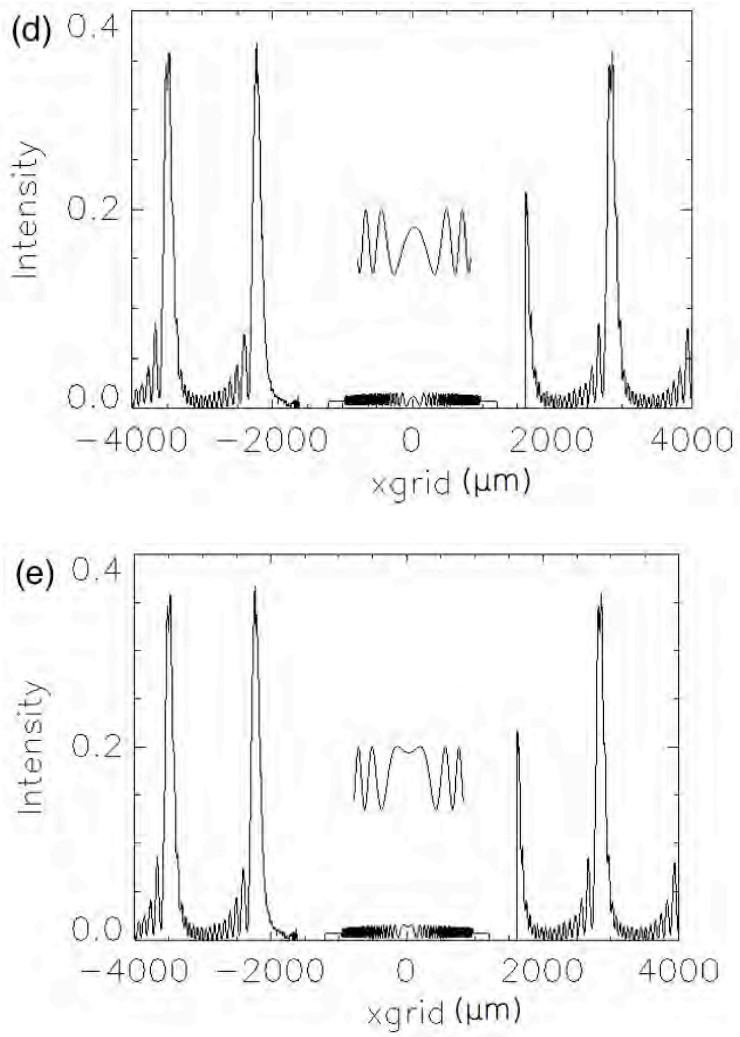

Figure 7: Intensity plots of the target at various temperatures. The center region is enlarged for clarity. (a) 18.73 K, (b) 18.43 K, (c) 18.09 K, (d) 17.70 K, (e) 17.23 K

The total shift as the temperature decreased from 18.73 K to 17.23 K was calculated to be 1.14 λ. It is also worth noting that the background interference does not change at all as temperature decreases, as any change in the index of refraction of the helium surrounding the target would be extremely small.

In the future, this result will be compared with the experimental results using an actual Fabry-Perot interferometer. If the experimental results match this theoretical result closely, then it would suggest that the target is cooling properly,

and has the gas density needed for ignition experiments on the NIF.

5. Conclusion

An experiment has been proposed that will use a Fabry-Perot interferometer to measure gas density changes inside a cryogenic target for use on the NIF. A program was written to model this experiment, taking many parameters into account. Using this program, plots were generated that predict the intensity for rays passing through the target, as well as through the helium gas surrounding it. These plots were generated at different temperatures to predict how deposition of gas and the resulting gas density drop would affect the optical path of rays traveling through the center of the target. This result will be compared with the experimental result in the future, and agreement between the two would indicate the readiness of current target designs for use on the NIF.

6. Acknowledgements

I would like to thank the following: Mr. Paul Sedita for encouraging my pursuit of physics and encouraging me to apply to the high school program at the LLE, Mr. Mark Wittman for his insight and advice, my parents for their love and support while I worked at the LLE, and the Laboratory for Laser Energetics and the University of Rochester for making this program possible. I would like to especially thank Dr. R. S. Craxton for his help and guidance, and for providing me with a wonderful learning opportunity.

References

[1] P.C. Souers, “Hydrogen Properties for Fusion Energy,” University of California Press. Print. (1986)

[2] M. Born and E. Wolf, “Principles of Optics: Electromagnetic Theory of Propagation, Interference, and Diffraction of Light,” Pergamon Press. Print. (1975)

[3] J. Y. Lee et al., “Spatiospectral transmission of a plane-mirror Fabry-Perot interferometer with nonuniform finite-size diffraction beam illuminations,” J. Opt. Soc. Am. A. **19**, 973-983 (2002)

[4] S. Jin, “A Ray-Tracing Model for Cryogenic Target Uniformity,” Laboratory for Laser Energetics High School Summer Research Program (2002), LLE Report 329

[5] Rogue Wave Software, Boulder, CO 80301

[6] Y. Yoshida et al., “Fabry-Perot Resonator with Slightly Tilted Mirrors,” Japan. J. Appl. Phys. **8**, 285-286 (1969).